Extended Phonon Collapse and the Origin of the Charge-Density Wave in $2H$-$NbSe_2$

F. Weber,[1,2,*] S. Rosenkranz,[1] J.-P. Castellan,[1] R. Osborn,[1] R. Hott,[2] R. Heid,[2] K.-P. Bohnen,[2] T. Egami,[3] A. H. Said,[4] and D. Reznik[2,5]

[1]*Materials Science Division, Argonne National Laboratory, Argonne, Illinois 60439, USA*
[2]*Karlsruher Institut für Technologie, Institut für Festkörperphysik, P.O.B. 3640, D-76021 Karlsruhe, Germany*
[3]*Department of Materials and Engineering, University of Tennessee, Knoxville, Tennessee 37996, USA*
[4]*Advanced Photon Source, Argonne National Laboratory, Argonne, Illinois 60439, USA*
[5]*Department of Physics, University of Colorado at Boulder, Boulder, Colorado 80309, USA*

(Received 29 March 2011; published 1 September 2011)

We report inelastic x-ray scattering measurements of the temperature dependence of phonon dispersion in the prototypical charge-density-wave (CDW) compound $2H$-$NbSe_2$. Surprisingly, acoustic phonons soften to zero frequency and become overdamped over an extended region around the CDW wave vector. This extended phonon collapse is dramatically different from the sharp cusp in the phonon dispersion expected from Fermi surface nesting. Instead, our experiments, combined with *ab initio* calculations, show that it is the wave vector dependence of the electron-phonon coupling that drives the CDW formation in $2H$-$NbSe_2$ and determines its periodicity. This mechanism explains the so far enigmatic behavior of CDW in $2H$-$NbSe_2$ and may provide a new approach to other strongly correlated systems where electron-phonon coupling is important.

DOI: 10.1103/PhysRevLett.107.107403 PACS numbers: 78.70.Ck, 63.20.dd, 71.30.+h, 71.45.Lr

The origin of charge-density-wave (CDW) order is a long-standing problem relevant to a number of important issues in condensed matter physics, such as the role of stripes in cuprate superconductivity [1] and charge fluctuations in the colossal magnetoresistive manganites [2]. Static CDW order, i.e., a periodic modulation of the electronic density, reflects an enhancement of the dielectric response of the conduction electrons at the CDW wave vector $\mathbf{q}_{\mathrm{CDW}}$, but it has long been known that it is stabilized only by a coupling to the crystal lattice [3,4]. Transitions into the CDW phase on lowering the temperature are accompanied by a softening of an acoustic phonon at $\mathbf{q}_{\mathrm{CDW}}$ to zero frequency at T_{CDW} where it freezes into a static distortion [5] and evolves into the new periodic (often incommensurate) superstructure. Chan and Heine derived the criterion for a stable CDW phase with a modulation wave vector $\mathbf{q}$ as [4]

$$\frac{4\eta_q^2}{\hbar\omega_{\mathrm{bare}}} \geq \frac{1}{\chi_q} + (2\bar{U}_q - \bar{V}_q), \tag{1}$$

where η_q is the electron-phonon coupling (EPC) associated with a mode at an unrenormalized energy of ω_{bare}, χ_q is the dielectric response of the conduction electrons, and $\bar{U}_q$ and $\bar{V}_q$ are their Coulomb and exchange interactions, respectively. Although both sides of this inequality are essential in stabilizing the CDW order, the common assumption is that the modulation wave vector $\mathbf{q}_{\mathrm{CDW}}$ is determined by the right-hand side, i.e., by a singularity in the electronic dielectric function χ_q at $\mathbf{q}_{\mathrm{CDW}} = 2\mathbf{k}_F$ ($\mathbf{k}_F$ is the Fermi wave vector).

In the case of $2H$-$NbSe_2$, it was proposed that such a singularity resulted either from direct Fermi surface nesting at $\mathbf{q}_{\mathrm{CDW}}$ [3,6] or from the presence of saddle points near the Fermi surface connected by $\mathbf{q}_{\mathrm{CDW}}$ [7]. However, this has been challenged by several theoretical investigations [8–10] based on which a recent density-functional-theory calculation correctly predicted a CDW instability but without singularities in χ_q [11,12]. Experimentally, several angle-resolved photoemission spectroscopy investigations did not find a sharp Fermi surface nesting [13–16]. The longtime elusive CDW gap was finally observed; however, its precise magnitude and wave vectors are still controversial [16,17]. As a consequence, the elegant and intellectually compelling picture of CDW formation driven by Fermi surface nesting has been called into question [10,11,13]. The alternative possibility is that the CDW transition in $2H$-$NbSe_2$ may instead be driven by the left-hand side of Eq. (1), i.e., the wave vector dependence of the EPC η_q. A direct test of this conjecture by phonon spectroscopy is the subject of this Letter.

We have investigated discrepancies with the Fermi surface-nesting scenario by measuring the energies and linewidths of phonon excitations in $2H$-$NbSe_2$ as a function of temperature, comparing both to *ab initio* calculations. In particular, the phonon linewidth provides detailed information related to the Fermi surface. Our results demonstrate that the soft-phonon physics in $2H$-$NbSe_2$ does indeed deviate strongly from the conventional picture based on nesting [3,5] and that the EPC is primarily responsible for determining $\mathbf{q}_{\mathrm{CDW}}$.

Earlier inelastic scattering investigations of the phonon dispersion in $2H$-$NbSe_2$ were limited by weak neutron scattering intensities due to the small sample size [18–20] or restricted to room temperature [21]. To

overcome these constraints, we utilized high-resolution inelastic x-ray scattering, which allowed us to obtain measurements of the entire dispersion of the soft-mode branch over a wide temperature range. We used a high-quality single crystal sample of about 50 mg ($2 \times 2 \times 0.05$ mm^3) with a T_{CDW} of 33 K determined from the temperature dependence of the superlattice reflections [Fig. 1(e)] in agreement with previous results [18]. All inelastic x-ray scattering experiments were carried out on the XOR 30-ID HERIX beam line [22,23] at the Advanced Photon Source, Argonne National Laboratory. Data were fitted with damped harmonic oscillator functions convoluted with the experimental resolution. For more details on the instrumental setup and data analysis, see [24]. Here, we focus on the longitudinal acoustic phonon branch dispersing in the crystallographic (100) direction and crossing $\mathbf{q}_{\mathrm{CDW}} = (0.329, 0, 0)$ [18].

Figure 1 shows the temperature dependence of a soft-phonon mode at $\mathbf{q}_{hkl} = (0.325, 0, 0)$, close to the CDW wave vector $\mathbf{q}_{\mathrm{CDW}} = (0.329, 0, 0)$. At $T = 90$ K [Fig. 1(d)], the soft phonon at an energy of $\omega_q = 4.5$ meV has nearly equal intensity to the second phonon branch at 10 meV. Upon cooling, the intensity of the upper branch is suppressed due to the Bose factor, whereas the intensity of the soft phonon is enhanced by a factor of $1/\omega_q$ in the cross section as its energy ω_q is reduced. At $T = T_{\mathrm{CDW}}$, the elastic superstructure peak of the CDW phase dominates the spectrum [Fig. 1(b)], but we can still distinguish the critically damped phonon as a broad peak beneath the narrow elastic CDW peak. Well inside the CDW phase, the elastic superlattice reflection was too strong for any inelastic scattering to be observed at $\mathbf{q}_{\mathrm{CDW}}$ [Fig. 1(a)].

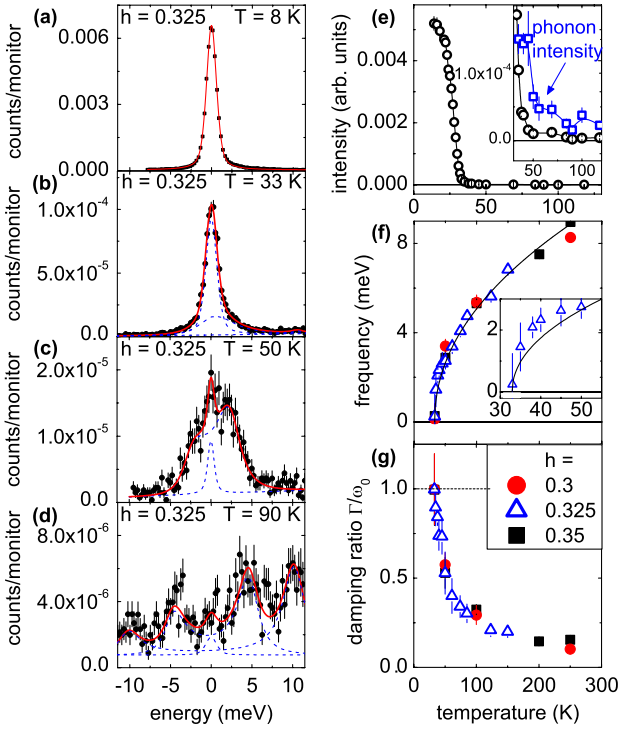

FIG. 1 (color online). Temperature dependence of the soft-phonon mode and the charge-density-wave superlattice peak near $q_{\mathrm{CDW}} = (0.329, 0, 0)$. (a)–(d) Energy scans at $\mathbf{q} = (3 - h, 0, 0)$, $h = 0.325$, for temperatures $8\ \mathrm{K} \leq T \leq 90\ \mathrm{K}$. Solid (red) lines are fits consisting of damped harmonic oscillators (inelastic) and a pseudo-Voigt function (elastic) (blue dashed lines). (e) Intensity of the charge-density-wave superlattice peak for $T \leq 120$ K. The inset shows the phonon and superlattice peak intensities just above T_c. (f),(g) Phonon frequency ω_q and critical damping ratio $\Gamma/\tilde{\omega}_q$ of the soft-phonon mode, respectively, at $\mathbf{q} = (h, 0, 0)$ with $h = 0.3$ (circle), 0.325 (triangle), and 0.35 (square). The solid line in (f) is a power law fit of the form $[(T - T_c)/T_c]^{\delta}$ yielding $\delta = 0.48 \pm 0.02$.

Figure 1(e) shows that the integrated intensity of the CDW superlattice peak measured at $h = 0.325$, which is within the momentum resolution of $\mathbf{q}_{\mathrm{CDW}}$, increases rapidly below $T_{\mathrm{CDW}} = 33$ K, in good agreement with previous neutron diffraction data taken on crystals from the same growth batch [18]. Above T_{CDW}, the elastic intensity due to diffuse scattering from the sample is very small, which implies that our sample had very little structural disorder. It stays low until very close to T_{CDW} [see the inset in Fig. 1(e)], where a weak elastic "central" peak consistent with low energy critical fluctuations appears.

The phonon energy at $\mathbf{q}_{\mathrm{CDW}}$ softens on cooling [Fig. 1(f)] following a power law $\omega_q(T) = [(T - T_c)/T_c]^{\delta}$ with $\delta = 0.48 \pm 0.02$, the value predicted by mean-field theory [3]. As the phonon softens, the damping increases and the phonon becomes critically damped, i.e., $\Gamma/\tilde{\omega}_q = 1$, at T_{CDW} [Fig. 1(f)].

Remarkably, we observe the same power law behavior not only at $\mathbf{q}_{\mathrm{CDW}}$ but also at $h = 0.3$ and 0.35, which are outside the experimental resolution from $\mathbf{q}_{\mathrm{CDW}}$ and where the elastic peak is an order of magnitude weaker relative to the phonon intensity. Moreover, the phonon energies at

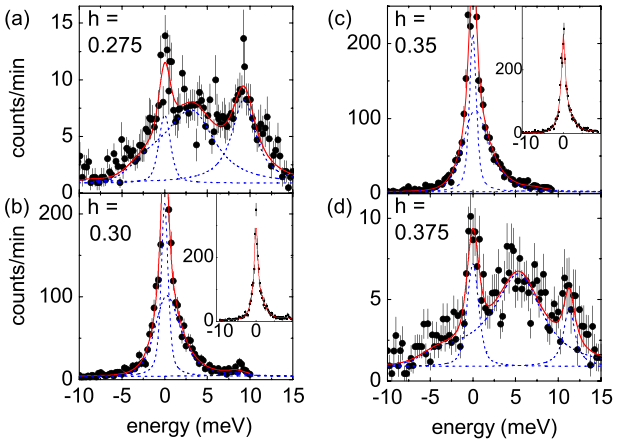

FIG. 2 (color online). Wave vector dependence of the soft phonon at $T = 33$ K. Energy scans at $\mathbf{Q} = (3 - h, 0, 1)$, $h = 0.275$–0.375. Solid (red) lines represent the total fit result consisting of a damped harmonic oscillator functions (inelastic) and a pseudo-Voigt function (elastic) (blue dashed lines).

these wave vectors also become indistinguishable from zero at T_{CDW} [Figs. 2(b) and 2(c)] as at $\mathbf{q}_{CDW}$. This means that the phonons are critically damped over a large range of momentum transfer from $h = 0.3$ to $h = 0.35$. Going further away from $\mathbf{q}_{CDW}$ with the same step size, $\Delta h = 0.025$ r.l.u., the soft-phonon branch is well separated from zero energy [Figs. 2(a) and 2(d)]. Figure 3 shows the full dispersion and damping ratio of the soft-mode phonon branch. A broad dispersion anomaly is already evident at 250 K in agreement with previous neutron scattering measurements performed only at 300 K [18]. This anomaly deepens considerably upon cooling to 50 K, where we also observe a strong increase in the damping. Finally, upon cooling to T_{CDW}, the energies reach zero and the phonons become critically damped over an extended range of wave vectors. At $T = 8$ K, well below T_{CDW}, we find hardened energies and reduced damping, similar to the ones observed at $T = 50$ K. However, the soft mode was not resolvable at $h = 0.325$ and 0.35 due to strong elastic scattering [e.g., see Fig. 1(a)]. At these temperatures, the Bose and $1/\omega$ factors suppress the phonon intensity and the measurements become increasingly difficult.

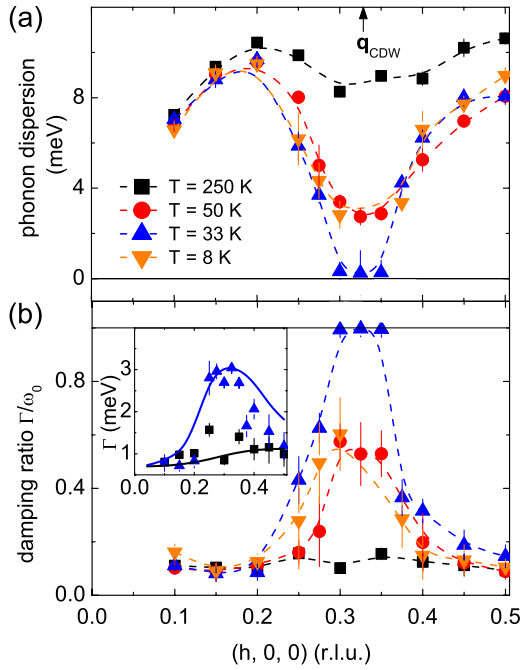

FIG. 3 (color online). Experimentally obtained dispersion and damping ratio of the soft-phonon branch in $2H$-$NbSe_2$ at four temperatures 8 K $\leq T \leq$ 250 K. Plotted are (a) the frequency of the damped harmonic oscillator $\omega_q = \sqrt{\tilde{\omega}_q^2 - \Gamma^2}$ and (b) the damping ratio $\Gamma/\tilde{\omega}_q$. Lines are guides to the eye. Note that phonons at $h = 0.325, 0.35$ and $T = 8$ K were not detectable due to strong elastic intensities. The inset in (b) shows the experimentally observed damping Γ of the damped harmonic oscillator (symbols) and scaled DFPT calculations (see Fig. 4) of 2γ (lines, offset 0.7 meV) with $\sigma = 0.1$ eV (black) and 1 eV (red).

The $\mathbf{q}$ dependence of the phonon softening shown in Fig. 3 is in marked contrast to the sharp, cusplike dips that normally characterize Kohn anomalies at $2\mathbf{k}_F$ due to Fermi surface nesting [5,25]. In $2H$-$NbSe_2$, we find that the phonon renormalization extends over 0.36 Å^{-1}, or over half the Brillouin zone, and the critically damped region extends over 0.09 Å^{-1}, whereas we can clearly determine different phonon energies at wave vectors separated by half of this value ($\Delta h = 0.025$ r.l.u. $= 0.045$ Å^{-1}). This behavior clearly rules out a singularity in the electronic response in $2H$-$NbSe_2$ and suggests that the CDW is determined by the wave vector dependence of the EPC η_q, as proposed by theory [9–11]. A broadened or even flat-topped susceptibility due to imperfect nesting caused, e.g., by the c-axis dispersion of the electron bands, could also lead to a renormalization of the phonon dispersion over a larger range of wave vectors, but it is unlikely that it spans over half of the Brillouin zone.

In order to elucidate the microscopic mechanism behind the CDW phase transition in $2H$-$NbSe_2$, we compare our experimental results to detailed phonon calculations based on density functional perturbation theory (DFPT) performed with the crystal structure at $T > T_{CDW}$ (for details see [24]). This is a zero temperature technique, in which structural instabilities show up as imaginary phonon frequencies. Because of the finite momentum mesh used in the DFPT calculations, a numerical smearing σ of the electronic bands is necessary to compare the calculations with experiment. The effect of σ is analogous to a thermal smearing of the electronic structure, so it has been used in previous work to qualitatively simulate the effect of temperature [25,26]. Though temperatures equivalent to σ are at least 1 order of magnitude too large (for details see [24]), we note that for $2H$-$NbSe_2$ a comparison between theory and experiment indicates that values of 0.1 eV $\leq \sigma \leq$ 1 eV produce results that are consistent with a temperature range of 30 K $\leq T \leq$ 300 K.

Figure 4 summarizes the calculations, showing the calculated soft-phonon dispersion, linewidth, and electronic joint density of states (JDOS). Imaginary phonon energies are represented in Fig. 4(a) through the negative roots of the absolute value, e.g., as "negative" phonon energies. These occur in the calculated longitudinal acoustic phonon branch for $\sigma \geq 0.18$ eV over an extended range of wave vectors [Fig. 4(a)] in agreement with previous studies [12] and in qualitative agreement with the observed breakdown of the phonon dispersion. Similarly, the contribution to the phonon linewidth from the electron-phonon interaction, 2γ [Fig. 4(b)], shows a strong enhancement over the same extended range of wave vectors. To a first approximation, 2γ is proportional to the product of $|\eta_{\mathbf{q}}|^2$ and the electronic JDOS. Since the latter shows negligible wave vector dependence [Fig. 4(c)], the enhancement of the phonon linewidth observed in both experiment and theory is entirely due to a strong wave vector dependence of the EPC.

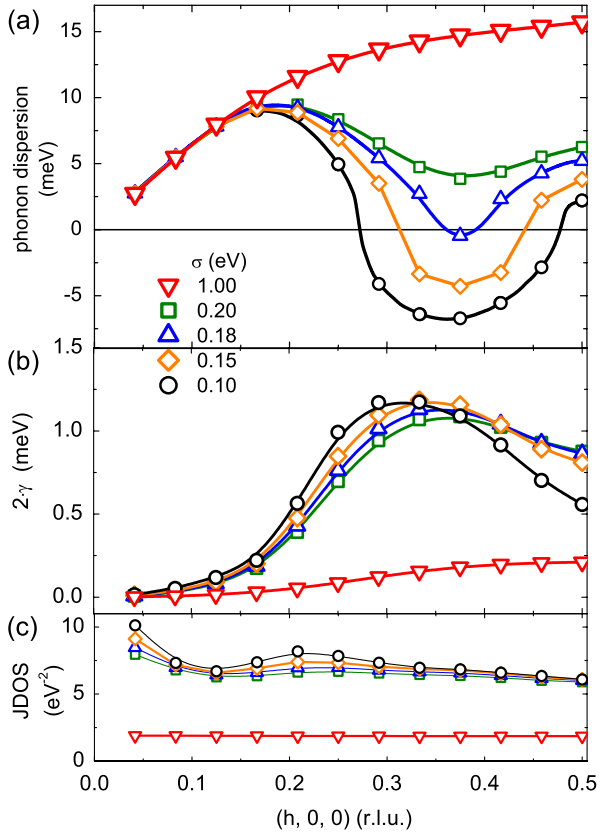

FIG. 4 (color online). *Ab initio* calculation for the soft-phonon mode along the crystallographic (100) direction in $2H$-$NbSe_2$. Shown are the calculated (a) dispersion, (b) 2γ [the contribution of the EPC to the phonon linewidth (FWHM)], and (c) the electronic JDOS. Calculations were done with $0.1\ \text{eV} \leq \sigma \leq 1.0\ \text{eV}$ (see the text). Note that calculated imaginary frequencies are shown as negative roots of the square phonon frequencies. Lines are guides to the eye.

Moreover, this range of strongly enhanced EPC is identical to the range over which the phonon softens. In contrast, the real part of χ shows a much broader and only very shallow peak [8,11]. Experimentally, conclusions differ depending on whether warping of the Fermi surface along $\mathbf{k}_z$ is taken into account [13] or neglected [15]. But even in the latter scenario, which yields a less broadened peak in $\text{Re}\chi$ at $h < 0.3$, the $\mathbf{q}$ dependence of $\text{Re}\chi$ cannot explain the observed phonon renormalization (for more details see [24]). This leads us to conclude that the observed $\mathbf{q}$ dependence of the phonon self-energy is entirely due to the EPC and that the CDW wave vector in $2H$-$NbSe_2$ is indeed determined by the left-hand side of Eq. (1).

Since our measurements demonstrate that Fermi surface nesting does not play a role in the CDW phase transition in $2H$-$NbSe_2$, the electronic states serve only to provide an elevated dielectric response, with the modulation wave vector entirely determined by the coupling between electronic and vibrational dynamics. Previous studies of chromium [27] and ruthenium [28] have shown that matrix elements can indeed sharply depend on the wave vector and also produce dips in the phonon dispersions, although in these compounds phonons do not soften to zero energy. Our work provides direct evidence that the same effect can drive the structural instability in a CDW compound. This result naturally explains why electronic probes do not find strong nesting at $\mathbf{q}_{\text{CDW}}$ in $2H$-$NbSe_2$. Our results have implications for many other strongly correlated systems. In particular, CDW correlations in the form of stripes and/or checkerboard patterns have been linked to the emergence of unusual states and physical properties, such as colossal magnetoresistance in the manganites [29] and the pseudogap state in the cuprates [30]. Indeed, the observation of phonon anomalies in manganites at the wave vector of the checkerboard-type order [31] and anomalies observed in $La_{2-x}Sr_xCuO_4$ at the stripe ordering wave vector [32] demonstrate that strong EPC could be important in these materials as well.

In conclusion, we reported inelastic x-ray measurements of the temperature dependence of a longitudinal acoustic phonon in $2H$-$NbSe_2$ involving the CDW soft mode. We observe an extended region in $\mathbf{q}$ with overdamped phonons at the CDW transition temperature. A detailed comparison to lattice dynamical calculations via DFPT shows that in $2H$-$NbSe_2$, the periodicity, i.e., $\mathbf{q}_{\text{CDW}}$, of the CDW ordered state is determined entirely by the wave vector dependence of the EPC. This is in stark contrast to the standard view that a divergent electronic response defines $\mathbf{q}_{\text{CDW}}$ and is evidence that a wave-vector-dependent EPC can drive a structural phase transition.

We acknowledge valuable discussions with I. Mazin, J. van Wezel, M. Norman, and D. Dessau. We thank J. M. Tranquada for supplying us with a single crystal of $2H$-$NbSe_2$. Work at Argonne was supported by U.S. Department of Energy, Office of Science, Office of Basic Energy Sciences, under Contract No. DE-AC02-06CH11357. The construction of HERIX was partially supported by the NSF under Grant No. DMR-0115852.

*frank.weber@kit.edu

[1] S. A. Kivelson, I. P. Bindloss, E. Fradkin, V. Oganesyan, J. M. Tranquada, A. Kapitulnik, and C. Howald, Rev. Mod. Phys. **75**, 1201 (2003).
[2] E. Dagotto, Science **309**, 257 (2005).
[3] G. Grüner, Rev. Mod. Phys. **60**, 1129 (1988).
[4] S. K. Chan and V. Heine, J. Phys. F **3**, 795 (1973).
[5] M. Hoesch, A. Bosak, D. Chernyshov, H. Berger, and M. Krisch, Phys. Rev. Lett. **102**, 086402 (2009).
[6] J. Wilson, Phys. Rev. B **15**, 5748 (1977).
[7] T. M. Rice and G. K. Scott, Phys. Rev. Lett. **35**, 120 (1975).
[8] N. J. Doran, B. Ricco, M. Schreiber, D. Titterington, and G. Wexler, J. Phys. C **11**, 699 (1978).
[9] N. J. Doran, J. Phys. C **11**, L959 (1978).

[10] C. M. Varma and A. L. Simons, Phys. Rev. Lett. **51**, 138 (1983).
[11] M. D. Johannes, I. I. Mazin, and C. A. Howells, Phys. Rev. B **73**, 205102 (2006).
[12] M. Calandra, I. I. Mazin, and F. Mauri, Phys. Rev. B **80**, 241108 (2009).
[13] K. Rossnagel, O. Seifarth, L. Kipp, M. Skibowski, D. Voß, P. Krüger, A. Mazur, and J. Pollmann, Phys. Rev. B **64**, 235119 (2001).
[14] D. W. Shen, Y. Zhang, L. X. Yang, J. Wei, H. W. Ou, J. K. Dong, B. P. Xie, C. He, J. F. Zhao, B. Zhou, M. Arita, K. Shimada, H. Namatame, M. Taniguchi, J. Shi, and D. L. Feng, Phys. Rev. Lett. **101**, 226406 (2008).
[15] D. S. Inosov, V. B. Zabolotnyy, D. Evtushinsky, A. Kordyuk, B. Buechner, R. Follath, H. Berger, and S. Borisenko, New J. Phys. **10**, 125027 (2008).
[16] S. Borisenko, A. Kordyuk, V. Zabolotnyy, D. Inosov, D. Evtushinsky, B. Büchner, A. Yaresko, A. Varykhalov, R. Follath, W. Eberhardt, L. Patthey, and H. Berger, Phys. Rev. Lett. **102**, 166402 (2009).
[17] K. Rossnagel (private communication).
[18] D. E. Moncton, J. D. Axe, and F. J. DiSalvo, Phys. Rev. Lett. **34**, 734 (1975).
[19] C. Ayache, R. Currat, and P. Molinie, Physica (Amsterdam) **180B–181B**, 333 (1992).
[20] K. Schmalzl, D. Strauch, A. Hiess, and H. Berger, J. Phys. Condens. Matter **20**, 104240 (2008).
[21] B. M. Murphy, H. Requardt, J. Stettner, J. Serrano, M. Krisch, M. Mueller, and W. Press, Phys. Rev. Lett. **95**, 256104 (2005).
[22] A. H. Said, H. Sinn, and R. Divan, J. Synchrotron Radiat. **18**, 492 (2011).
[23] T. S. Toellner, A. Alatas, and A. H. Said, J. Synchrotron Radiat. **18**, 605 (2011).
[24] See Supplemental Material at http://link.aps.org/supplemental/10.1103/PhysRevLett.107.107403 for details regarding experimental setup, data analysis, and density functional calculations and for a detailed discussion of the influence of the electronic susceptibility χ on the phonon renormalization in $2H$-$NbSe_2$.
[25] K.-P. Bohnen, R. Heid, H. J. Liu, and C. T. Chan, Phys. Rev. Lett. **93**, 245501 (2004).
[26] L. Pintschovius, F. Weber, W. Reichardt, A. Kreyssig, R. Heid, D. Reznik, O. Stockert, and K. Hradil, Pramana **71**, 687 (2008).
[27] D. Lamago, M. Hoesch, M. Krisch, R. Heid, K.-P. Bohnen, P. Boni, and D. Reznik, Phys. Rev. B **82**, 195121 (2010).
[28] R. Heid, L. Pintschovius, W. Reichardt, and K.-P. Bohnen, Phys. Rev. B **61**, 12 059 (2000).
[29] S. Cox, J. Singleton, R. D. Mcdonald, A. Migliori, and P. B. Littlewood, Nature Mater. **7**, 25 (2007).
[30] A. Damascelli, Z. Hussain, and Z.-X. Shen, Rev. Mod. Phys. **75**, 473 (2003).
[31] F. Weber, N. Aliouane, H. Zheng, J. F. Mitchell, D. N. Argyriou, and D. Reznik, Nature Mater. **8**, 798 (2009).
[32] D. Reznik, L. Pintschovius, M. Ito, S. Iikubo, M. Sato, H. Goka, M. Fujita, K. Yamada, G. D. Gu, and J. M. Tranquada, Nature (London) **440**, 1170 (2006).